THE JOURNAL OF COMPARATIVE NEUROLOGY 504:570–582 (2007)

The *foraging* Gene of *Drosophila melanogaster:* Spatial-Expression Analysis and Sucrose Responsiveness

A.T. BELAY,[1] R. SCHEINER,[2] A.K.-C. SO,[1] S.J. DOUGLAS,[1]
M. CHAKABORTY-CHATTERJEE,[1] J.D. LEVINE,[1] AND M.B. SOKOLOWSKI[1]*
[1]Department of Biology, University of Toronto, Mississauga, Ontario L5L 1C6, Canada
[2]Institut für Ökologie, Technische Universität Berlin, D-10587 Berlin, Germany

ABSTRACT

The ability to identify and respond to food is essential for survival, yet little is known about the neural substrates that regulate natural variation in food-related traits. The *foraging* (*for*) gene in *Drosophila melanogaster* encodes a cGMP-dependent protein kinase (PKG) and has been shown to function in food-related traits. To investigate the tissue distribution of FOR protein, we generated an antibody against a common region of the FOR isoforms. In the adult brain we localized FOR to neuronal clusters and projections including neurons that project to the central complex, a cluster within the dorsoposterior region of the brain hemispheres, a separate cluster medial to optic lobes and lateral to brain hemispheres, a broadly distributed frontal-brain cluster, axon bundles of the antennal nerve and of certain subesophageal-ganglion nerves, and the medulla optic lobe. These newly described tissue distribution patterns of FOR protein provide candidate neural clusters and brain regions for investigation of neural networks that govern foraging-related traits. To determine whether FOR has a behavioral function in neurons we expressed UAS-*for* in neurons using an *elav-gal4* driver and measured the effect on adult sucrose responsiveness (SR), known to be higher in rovers than sitters, the two natural variants of *foraging*. We found that pan-neuronal expression of *for* caused an increase in the SR of sitters, demonstrating a neural function for PKG in this food-related behavior. J. Comp. Neurol. 504:570–582, 2007.
© 2007 Wiley-Liss, Inc.

Indexing terms: *for*; cGMP-dependent protein kinase; sucrose response; immunocytochemistry; *Drosophila melanogaster*

Studies of the fruit fly *Drosophila melanogaster* have uncovered genetic, molecular, and neural mechanisms underlying complex behaviors such as courtship, rhythms, learning, and memory (Hall, 2003). Behaviors such as sleep, aggression, food-related behaviors, and social dynamics have more recently joined the compendium of complex behaviors investigated in this species of insect (Sokolowski, 2001; Greenspan, 2004). Overall, studies performed using relatively simple models such as *Drosophila* provide us with principles for understanding elements of nervous-system development and function that underlie complex behaviors. Among the prospects so revealed is identification of candidate genes that potentially contribute to the control of analogous behaviors in other species, including mammalian ones (Fitzpatrick et al., 2005). Of particular interest to us are genes that influence natural variations in behavior and how they regulate relevant neuronal pathways.

Natural variation in the *foraging* (*for*) gene of *Drosophila* has furthered our understanding of larval and adult food-related behaviors (Osborne et al., 1997; Douglas et al., 2005). *for,* which is synonymous with the *dg2* gene

Grant sponsor: Canadian Institutes of Health Research; Grant numbers: MOP 57865 (to M.B.S.) and MOP 74665 (to J.D.L.); Grant sponsor: National Institutes of Health; Grant number: R01 DK70141 (to M.B.S.); Grant sponsor: Canada Research Chair Programme (to M.B.S. and J.D.L.); Grant sponsor: Canada Institutes of Health Research (training grants to A.T.B., A.K-C.S., and S.J.D.).

*Correspondence to: Marla B. Sokolowski, University of Toronto, 3359 Mississauga Rd., Mississauga, Ont. L5L 1C6, Canada.

E-mail: msokolow@utm.utoronto.ca

Received 18 December 2006; Revised 11 June 2007; Accepted 29 June 2007

DOI 10.1002/cne.21466

Published online in Wiley InterScience (www.interscience.wiley.com).

© 2007 WILEY-LISS, INC.

WILEY InterScience® DISCOVER SOMETHING GREAT

(Kalderon and Rubin, 1989), encodes a cGMP-dependent protein kinase (PKG). *For* is a large gene (encompassing >40 kb of genomic DNA) with three major transcripts called T1, T2, and T3 (T3 is an mRNA subset of T1) (Osborne et al., 1997). The functions of *for*'s transcripts in food-related behaviors have not been described. *for* has two naturally occurring alleles, rover (for^R) and sitter (for^s). Rovers have higher PKG enzyme activities (Osborne et al., 1997), longer larval foraging trails, and move more between food patches compared to sitters (Sokolowski, 1980). Rover and sitter locomotion does not significantly differ in the absence of food. The exact DNA sequence polymorphism(s) responsible for the rover/sitter differences in behavior have not yet been identified.

for also affects adult food-related behaviors. Adult rovers walk farther from a sucrose drop postfeeding (Pereira and Sokolowski, 1993), have higher sucrose responsiveness (SR), and take longer to habituate to repeated presentations of sucrose than sitters or sitter mutants (Scheiner et al., 2004b). The neural components of these phenotypes have not been investigated primarily due to the elusive nature of good *Drosophila* FOR antibodies. We developed an antibody to study FOR protein expression in the head of the fly and found that FOR is mostly localized in clusters of neurons in the adult brain.

We investigated SR, one of the previously mentioned *for*-related phenotypes, as a means to discover whether FOR acts in neurons to affect variation in food-related behaviors. In insects, SR is thought to be an indicator of general sensory acuity. For example, in the honeybee, SR correlates with responsiveness to odors and visual stimuli (Scheiner et al., 2004a; Erber et al., 2006), nonassociative and associative learning ability (Scheiner et al., 1999, 2001a,b, 2005; Scheiner, 2004) and foraging behavior. In the fruitfly, SR is measured by stimulating the front tarsi of the leg of a fly with a sucrose solution. Sucrose stimuli are perceived by gustatory receptors on the front tarsi which project into the thoraco-abdominal ganglia (Stocker, 1994; Singh, 1997). When the sucrose is of sufficient concentration, the fly extends its mouth part in a proboscis extension response (PER) (Dethier, 1955).

We investigated neural requirements of FOR in SR. We expressed *for* in neurons because our immunohistochemical analysis showed that FOR was primarily found there. We increased the expression of *for* in sitters and tested for rover-like SR since sitter heads have lower PKG enzyme activities than rover heads (Osborne et al., 1997). Specifically, we used a pan-neuronal GAL4 driver (*elav-gal4*) to determine whether expression of the major *for* transcripts (*forT1* and *T2*) in the nervous system is sufficient to increase sitter SR to a rover-like level. Both the *forT1* and *T2* transgenes were able to increase SR when expressed in an *elav-gal4* pattern, although *forT2* caused a greater increase in SR than *T1*. The neural expression pattern of FOR combined with the behavioral results provide insight into the cellular mechanisms of FOR in sucrose responsiveness and provide candidate brain regions that may mediate FOR's functions in other food-related behaviors.

MATERIALS AND METHODS

Fly strains

Drosophila melanogaster were maintained in 170-mL bottles with 40 mL of yeast-sucrose-agar medium at 25 ± 1°C, on a 12L:12D photocycle with lights on at 0800. The rover (for^R) and sitter (for^s) strains were homozygous for their for^R or for^s alleles, respectively. for^R and for^s also share a common pair of third chromosomes derived from for^R (de Belle and Sokolowski, 1987). for^{s2} is a sitter mutant generated on the rover (for^R) genetic background (de Belle et al., 1989; Pereira and Sokolowski, 1993). Other strains used in this study were the wildtype, *Canton S* (*CS*) strain, a recessive embryonic-lethal deletion-bearing strain, $Df(2L)drm^{P2}$, with left and right breakpoints at the second-chromosomal sites *l(2)k10101* and *l(2)k06860*, respectively (Green et al., 2002), and a homozygous, pupal-lethal deletion-bearing strain, *Df(2L)ED243*, custom-made using the Drosdel insertion lines *CB-0383-3* and *5-HA-2002* (Ryder et al., 2004). This deletion removes 24,679 bp of chromosome 2L, from 3,632,218 bp to 3,656,897 bp that correspond to the first four exons of the T1 transcript and the first two exons of the T3 transcript. Also, 210 bp of the first exon of T2 is removed by this deletion, which does not include the start codon. Reverse-transcriptase polymerase chain reaction (RT-PCR) and Western blot analysis using extracts collected from homozygous mutant larval tissues showed that T1- and T3-specific isoforms are absent in this deletion line, while T2-specific isoforms are reduced but not knocked out (data not shown). *DSK001* is used as control for the *Df(2)ED243* mutant strain and is the parental strain used to generate the Drosdel insertion lines *CB-0383-3* and *5-HA-2002*.

A pan-neuronal driver, *elav-gal4* (Lin and Goodman, 1994) and the transgenic strains *UAS-mCD8-GFP* (Bloomington Stock Center, Bloomington, IN) were used in histological studies. To generate *for* transgenes, DNA fragments encoding the complete FORT1 and T2 proteins were obtained from the corresponding cDNA constructs, generated by D. Kalderon (Kalderon and Rubin, 1989). They were subcloned into the transformation vector pUAST (Brand and Perrimon, 1993) and transformed into $white^1$ (w^1) mutant embryos according to standard procedures (Spradling, 1986). We generated viable homozygous insertion strains UAS-*forT1* and UAS-*forT2* constructs and then crossed them into a for^s, genetic background (including the w^1 eye-color marker) to produce $w^1;for^s;$ UAS-*forT1* and $w^1;for^s;$UAS-*forT2*, respectively. To express *forT1* and *forT2* in the nervous system of sitters, we separately crossed the $w^1;for^s;$UAS-*forT1* and $w^1;for^s;$ UAS-*forT2* lines to a $w^1;for^s;elav\text{-}gal4$ line. Negative controls were generated by crossing $w^1;for^s$ to each of $w^1;for^s;$ UAS-*forT2*, $w^1;for^s;$UAS-*forT1*, and $w^1;for^s;elav\text{-}gal4$.

PKG enzymatic activity assay

PKG enzyme assays (modified from Osborne et al., 1997) were performed on 4–7-day-old adult head and body homogenates of for^R, for^s, and for^{s2}. Twenty heads or 10 bodies were homogenized in 25 mM Tris (pH 7.4), 1 mM EDTA, 2 mM EGTA, 0.05% Triton X-100, 5 mM b-mercaptoethanol, and protease inhibitor cocktail (Roche Diagnostics, Indianapolis, IN) and microcentrifuged for 5 minutes at 4°C. The supernatant was then removed and a subset was used to determine the total protein amount using BioRad Protein Assay Reagent (Bio-Rad Laboratories, Hercules, CA). Supernatants containing equal amounts of total protein were analyzed for PKG activity. This was done in a 70 μL reaction mixture containing (at final concentration): 40 mM Tris-HCl (pH 7.4), 20 mM magnesium acetate, 0.2 mM [γ^{32}P]ATP (500–1,000 cpm/

TABLE 1. Oligonucleotides Used for PCR Amplification of *for* Coding Sequences

Primer Designation	Primer Sequence (5′ → 3′)	cDNA clone ID #
CTf	TGGATCCATGGCTCCTATTGG	GH10421
CTr	CGGATCCCGGACCCTCAG	
T1f	CAAGCTTATGCGTTTCTGC	LD46758
T1r	AAAGCTTAGAGAGCATCG	
T2f	ACTCGAGTCTTTCGTAATG	GH10421
T2r	ACTCGAGTCAGAAGTCCT	
T3f	GAAGCTTATGCAGAGTCTG	LD46758
T3r	AAAGCTTAGAGAGCATCG	

Forward (f) and reverse (r) primers were designed from cloned *for* cDNA sequences reported by Flybase. Nucleotide substitutions were made in the primers to introduce restriction sites (underlined) that would facilitate subsequent cloning and recombinant PKG expression. T1, T2, T3 represent the three *for* isoforms; CT represents primer sequence common to all of the *for* transcripts.

pmol) (Amersham Pharmacia Biotech, Piscataway, NJ), 113 μg/mL heptapeptide (RKRSRAE) and 3 μM c-GMP (Promega, Madison, WI), and a highly specific c-AMP dependent protein kinase A (PKA) inhibitor (4.6 nM) (5-24, Calbiochem, La Jolla, CA). As a control, reactions were performed in the presence of 468 nM PKG inhibitor K-5823 (Calbiochem). The reaction mixtures were incubated at 30°C for 10 minutes, followed by termination of the reaction by spotting 70 μL of the reaction mix onto Whatman P-81 filters, which were then soaked with 75 mM H_3PO_4 for 5 minutes and washed three times with 75 mM H_3PO_4 to remove any unreacted [γ^{32}P]ATP. Filters were rinsed with 100% ethanol and air-dried before quantification. For quantification of PKG activity, counts were taken in a Wallac 1409 Liquid Scintillation Counter (PerkinElmer, Boston, MA) using universal scintillation cocktail (ICN). Specific activity of PKG was expressed as pmol of ^{32}P incorporated into the substrate per minute per mg protein.

Recombinantly produced FOR oligopeptide and antibody production

Recombinant forms of PKG were generated in *E. coli* by using two different expression systems. For the generation of PKG-specific antibodies, a C-terminal 40-aa segment, DGFYWWGLQNCTLEPPIKPAVKSVVDTTNFDDYPPDPEGP, that is common to the deduced proteins from each of the three major *for* transcripts (Kalderon and Rubin, 1989) was identified by sequence alignment. Additional alignments showed that this C-terminal segment is specific to these *for* expression products and is not encoded by any other sequences in the *Drosophila* genome. A 133-bp DNA fragment encoding this PKG-specific segment was subsequently amplified by the PCR from a *for* T2 cDNA clone (ID #GH10421) kindly provided by the Canadian *Drosophila* Microarray Centre (CDMC, University of Toronto). Amplifications were performed using engineered primers (Table 1, CTf/CTr primer) and AmpliTaq DNA polymerase (PerkinElmer) under the following conditions: 94°C initial denaturation for 2 minutes; 35 cycles of 94°C for 25 seconds, 55°C for 25 seconds, 72°C for 20 seconds; 72°C final extension for 5 minutes. The amplicon was digested with *Bam*HI and the resulting restriction fragment was ligated into the corresponding site of the pGEX-3X expression vector (Amersham). This plasmid construct, which encodes a GST-PKG fusion protein, was subsequently electrotransformed and maintained in *E. coli* BL21(DE3) cells (Novagen, Madison, WI) using standard techniques (Sambrook and Russell, 2001).

Induced expression of the GST-FOR fusion protein in 1-L bacterial cultures was carried out by the addition of 1 mM isopropyl-β-D-thiogalactoside, as previously described (So and Espie, 1998). To improve the solubility of the expressed GST-FOR protein, lysates were supplemented with 1% (w/v) sarkosyl and maintained at 4°C with gentle swirling for 10 minutes. Affinity purification of the GST-FOR polypeptide was performed using glutathione-linked sepharose 4B (GE Healthcare, Madison, WI), according to the manufacturer's instructions. Eluted protein was quantified using the Bio-Rad Protein Assay dye reagent. Purified GST-FOR protein (1 mg) was emulsified with complete Freund's adjuvant and used to immunize rabbits and guinea pigs. Three subsequent boosts (0.5 mg antigen) with incomplete Freund's adjuvant were administered at 2-week intervals before terminal bleeds were collected. Prior to immunocytochemical and Western blot analyses the antisera were preincubated with nitrocellulose-bound GST to absorb and remove the antibodies generated against the GST portion of the antigen.

For validation of the anti-FOR antibodies, constructs were also generated for the expression of each FOR isoform encoded by the three major *for* transcripts. The entire T1, T2, and T3 coding sequences were amplified from cDNA clones (CDMC) using sequence-specific primers (Table 1) and the PCR conditions described above, except that the 72°C cycle and final extension times were increased to 2 and 10 minutes, respectively. The *Hin*dIII-digested *for* T1 and T3 fragments and the T2 *Xho*I fragment were each ligated into the pET-21b vector (Novagen) for the subsequent bacterial expression of epitope-tagged versions of the three FOR isoforms. Cloned DNA fragments were sequenced using an ABI Prism 373A Gene Analyzer (Foster City, CA) to confirm the correct sequence, orientation, and reading frame of the inserts.

Immunoblots

Samples containing soluble *Drosophila* protein (15 μg) from 3–7-day-old fly heads or epitope-tagged FOR (10 ng) prepared from *E. coli* (So et al., 2002) were separated by denaturing polyacrylamide gel electrophoresis and transferred onto BioTrace NT pure nitrocellulose (Pall, West Chester, PA) using the Bio-Rad Mini Trans-Blot system, as vendor recommended. To ensure consistent loading among lanes and proper transfer of protein onto the nitrocellulose membrane, the latter were stained with 0.2% Ponceau S (Sigma, St. Louis, MO) solution. Immunodetection of FOR protein on Western blots was carried out as in So and Espie (1998) using anti-FOR and horseradish peroxidase-conjugated goat antirabbit or antiguinea pig IgG (Jackson Immunological, West Grove, PA) at 1:1,000 and 1:10,000 (v/v) dilutions, respectively. Signals were detected using the ECL Plus Western Blotting Detection kit and the Storm 840 Imaging System (GE Healthcare).

Immunocytochemistry

Assessments of FOR immunoreactivity in situ were performed on whole-mount for^R, for^s, and for^{s2} adult male and female tissue. Because no strain or sex differences in the spatial distribution of FOR-immunoreactivity were observed we focused immunocytochemical analyses on adult for^R females (upwards of 50 brains were imaged). Brains were dissected in phosphate-buffered saline (PBS pH 7.4), fixed in 4% paraformaldehyde in PBS, washed several

times in PBS-TX (PBS with 0.5% Triton X-100), and blocked in 10% normal goat serum (Jackson ImmunoResearch), 0.1% bovine serum albumin (BSA) (Sigma) in PBS-TX for 2 hours at room temperature. Specimens were then incubated in primary antibody (anti-FOR raised in guinea pig 1:100) for 24–48 hours at 4°C, washed several times in 0.5% PBT, and then incubated in secondary antibody (diluted 1:100) for 24 hours at 4°C. We generated two rabbit and two guinea pig anti-FOR sera. All of these antibodies worked well on Westerns. Although anti-FOR raised in both guinea pig and rabbit produced clean results on Western blot studies, we found that one guinea pig anti-FOR produced stronger and cleaner staining in immunocytochemical studies.

Additional primary antisera used here have been described previously. Neuronal nuclear marker, mouse anti-ELAV, used in this study at 1:200 dilution (mAb Elav-978A9 concentrate, Developmental Studies Hybridoma Bank, University of Iowa, Iowa City, IA), was raised against a fusion protein of the first 260 amino acids of phage T7 and the full-length ELAV protein (O'Neill et al., 1994). This antiserum stains 50 kDa ELAV-specific bands on Western blot (for example, see Samson et al., 1995). Glia marker mouse anti-REPO (8D12 anti-Repo concentrate, Developmental Studies Hybridoma Bank) was raised against a fusion protein containing 6-histidine and amino acids 218–612 of *Drosophila* Repo protein (DSHB). This antibody (used in this study at 1:200) stains glia cells as shown by colocalization studies with known glia cell markers (Campbell et al., 1994; Halter et al., 1995). The neuropile marker mouse mAb nc82 (used at 1:20, a gift from A. Hofbauer) is an Ig-G produced by a hybridoma clone from a large library generated against *Drosophila* heads (Hofbauer, 1991; Rein et al., 1999; Wagh et al., 2006). It is widely used in confocal images of *Drosophila* brains, providing a structural framework for the "standard brain" (Rein et al., 1999). It recognizes two proteins of 190 and 170 kDa in Western blots of homogenized *Drosophila* heads (Wagh et al., 2006). Rat anti-mCD8 (used at 1:100, Caltag, South San Francisco, CA) is a monoclonal antibody generated against the mouse CD8 alpha subunit. This antibody is widely used to visualize transgenic expression and does not show staining in the brain in the absence of the transgenic construct mCD8 (data not shown).

Secondary antibodies used in this study were goat Cy2-, Cy3-, or Cy5-conjugated antimouse or antiguinea pig Ig (1:100 dilutions, Jackson ImmunoResearch). To control for nonspecific binding of secondary antibody, tissues were treated with secondary antibody, without preincubation with primary sera. As a further control the primary antibody (1:100 dilution) was preadsorbed overnight at 4°C with 100 μg of FOR peptide (the FOR antigen used for immunization) before incubation of specimens. Fluorescently labeled tissues were examined with an LSM 510 confocal laser scanning microscope (Zeiss, Thornwood, NY) and images were edited for contrast using Adobe Photoshop (San Jose, CA).

Sucrose responsiveness

The protocol for quantifying sucrose responsiveness (SR) has been described (Scheiner et al., 2004b). Briefly, flies were food-deprived in the presence of water for either 24 ± 0.5 or 2 ± 0.5 hours and individually placed into a cut pipette tip (0.5–20 μL, Th. Geyer, Berlin); one leg of the fly protruded from the tip. The tarsus of the leg was touched with a toothpick moistened with either water or sucrose concentrations ranging from 0.1%, 0.3%, 1%, 3%, 10%, 30% (weight/volume H_2O) and a proboscis extension was noted. Each fly was exposed in a pseudorandomized order in one of seven sequences which included water and the six sucrose concentrations listed above. Only the data from water-satiated flies, those that did not exhibit a proboscis extension to water, were analyzed. The total number of responses to the six different sucrose concentrations was called the sucrose response score (SRS), and it ranged from 0 to 6. Analysis of variance (ANOVA) was used to test for the effects of strain, sex, and food deprivation on SRS, and post-hoc pairwise comparisons were done using Scheffé Tests (Zar, 1999).

RESULTS

Antibodies against FOR recognize major isoforms of the protein

The neural substrates involved in adult food-related behavior in *Drosophila* are unknown. Because the expression pattern of endogenous FOR has not been described, we generated an antibody against the *for* gene products and used it to investigate the expression pattern of this PKG protein in various neural tissues by conducting a detailed study in the adult brain, as well as an overview of expression in sensory neurons within the antennae, foreleg tarsi, wings, and proboscis. The immunogen used was a 40 amino-acid fragment common to the C-terminus sequence of the three major FOR isoforms (T1, T2, and T3). Sequence alignments showed that this C-terminal segment is unique to *for* gene products and common to all FOR isoforms (data not shown).

The specificity of the FOR antibody was demonstrated by immunoblotting bacterially expressed, epitope-tagged FOR T1, T2, and T3 proteins. Three bands corresponding to the molecular weights of the three recombinant FOR isoforms (recombinant T1, T2, T3 with MW of 123.62, 104.13, and 85.62 kDa, respectively; Fig. 1A, lanes 2, 3, and 4) were observed demonstrating that anti-FOR can recognize FOR proteins. We then assayed the presence of FOR isoforms in the heads of wildtype (*Canton-S*) flies. We observed three bands corresponding to the predicted molecular weights of T1, T2, and T3 FOR isoforms (predicted MW 121, 101, and 83 kDa, respectively, and observed MW 120, 95, and 83 kDa, respectively; Fig. 1A, lane 1). A band corresponding to the predicted molecular weight of DG1 (87 kDa), a closely related PKG, was not observed (Kalderon and Rubin, 1989). To further validate the specificity of our anti-FOR antibody we assessed FOR expression in a deletion strain, $Df(2L)drm^{P2}$, which harbors a 165-Kb deletion removing part of the *for* locus (Green et al., 2002). Fly heads heterozygous for drm^{P2} (deletion-over-balancer chromosome) showed a reduction in the intensity of the three FOR isoform bands compared to the wildtype CS control strain (Fig. 1B). Together these findings show that the FOR antibody can recognize endogenous FOR proteins.

Although we have shown that rover and sitter heads differ in PKG activity (Osborne et al., 1997), it was not known if all FOR isoforms are expressed in their heads. To investigate this we used head protein extracts from for^{R},

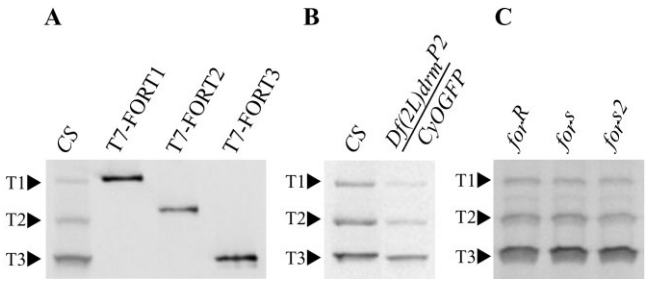

Fig. 1. Immunodetection of recombinant and endogenous forms of FOR protein using anti-FOR. **A:** Western blot containing protein extracted from wildtype (*CS*) heads and affinity-purified, recombinant (T7-tagged) forms of FOR isoforms (FOR-T1, FOR-T2, and FOR-T3) was developed using anti-FOR generated in guinea pigs. Anti-FOR recognizes the three T7-tagged FOR proteins (lanes 2, 3, and 4) as well as the three major isoforms of endogenous FOR (lane 1) from a wildtype (CS) head extract. **B:** Detection of FOR in the heads of deletion heterozygote mutant animals, for^{drmP2}/*CyOGFP*, and the wildtype control, *CS*. Compared to the wildtype control, the intensity of the three bands is reduced by half in head extracts of flies heterozygous for a *for*-minus deletion drm^{P2} and a second-chromosome (for^{+}-containing) balancer called *CyOGFP*. **C:** All three FOR isoforms (T1, T2, and T3) are expressed in for^{R}, for^{s}, and for^{s2} heads. This was also found for female heads (data not shown).

for^{s}, and for^{s2} and performed Western blots. We found that all three major isoforms of FOR are expressed in the heads of the natural for^{R} and for^{s} strains and the sitter mutant, for^{s2} (Fig. 1C). The for^{s2} mutation did not exhibit missing or aberrant sized isoforms.

Localization of FOR in the *D. melanogaster* brain

We used the antibody described above to investigate FOR expression patterns in the adult brain. We observed discreet clusters of FOR-immunoreactive (FOR-IR) cells in several regions of the adult brain (Fig. 2A,B). Some cells were in tight clusters while others were regionally restricted but distributed across a central-brain region (see result below). In addition, FOR-IR cells and fiber-like projections were found in the optic ganglia. To begin to examine the specificity of our antibody in adult tissues, we stained brains with a preincubated mixture of anti-FOR antiserum and FOR antigen (the antigen used to generate this antibody). Localized signal (Fig. 2A,B) was almost abolished when tissues were incubated with the preadsorbed antibody (Fig. 2C). The low level of background expression in the brain samples treated with the preadsorbed antibody is similar to that observed when tissues were stained in the absence of primary anti-FOR antibody (Fig. 2D).

As a further confirmation of specificity of anti-FOR immunolabeling, we used the FOR isoform-specific null deletion mutant *Df(2L)ED243* that is homozygous larval-viable but pupal lethal. In the control wildtype strain, *DSK001*, we found that FOR was localized to the larval proventriculus (PV), specifically as punctates throughout its outer epithelial cell layer (Fig. 2E). The proventriculus is part of the larval digestive system; it serves as a valve, regulating food passage into the midgut (Skaer, 1993). The punctate expression pattern of FOR observed in the PV of the *DSK001* control strain was completely absent in the homozygous deletion mutant *Df(2L)ED243* (Fig. 2F). Together, the results of the Western and immunocytochemical analyses show that the anti-FOR antiserum used here detects and is specific to endogenous FOR.

FOR immunoreactive cells are positive for a neuron-specific marker

Most if not all FOR-expressing cells are neurons, as determined by positive colocalization between the FOR-expressing cells and a nuclear neuronal marker, anti-ELAV (Figs. 3C″,E,G′,I′, 4B). All FOR-IR cells were ELAV-positive, with the exception of cells within the optic lobe medulla (Fig. 4E″). Single confocal sections showed that the FOR-IR crescent-like cells of the medulla are not ELAV positive (Fig. 4E,E′,E″). Furthermore, double labeling with anti-mCD8 and anti-FOR in strains expressing the reporter UAS-mCD8GFP driven by *elav-gal4* showed colocalization of these markers in the FOR-IR projections of the antennal nerve (data not shown). Immunostaining with a glial cell marker, anti-REPO (Campbell et al., 1994), indicated that FOR did not colocalize with glia (data not shown) in any of the FOR-IR regions including the medulla.

FOR-immunoreactive cell clusters in the anterior CNS

We found five FOR-IR cell clusters within the anterior CNS and two immunoreactive projections.

FOR-IR cellular clusters.

Cluster #1: within the ellipsoid body. We observed groups of FOR-IR neurons dorsolateral to the antennal lobes (Fig. 3A,B). In this cluster, FOR is localized to the nucleus and shows colocalization with the neural marker anti-ELAV (Fig. 3C,C′,C″). The cells are in close proximity to each other within each cluster and hence appear to be intensely stained. We counted an average of 27 ± 3 ($n = 6$) neurons per hemi-brain. Interestingly, these neurons give rise to neurites that can be traced to the neuropiles of the central complex (CC); however, these projections do not stain as strongly as the cell bodies (Fig. 3A). The ellipsoid body (EB) is a doughnut-shaped midline structure and is part of the centrally located CC. It is thought to be an integration center of the brain for processes such as locomotor behavior and learning (Heisenberg, 1994; Strauss, 2002). The EB was previously implicated in foraging behavior using structure-function analysis (Varnam et al., 1996). Images of this FOR-IR region taken at higher magnification show that the cell bodies are situated at the anterior region of the brain (Fig. 3B) while sending projections posteriomedially to the EB. The position and morphology of these cells resembles that reported for the large-field and small-field neurons that innervate the EB (Renn et al., 1999) and are thought to interconnect the different subunits of the CC.

Cluster #2: dorsoposterior. Bilateral clusters of 4–5 FOR-IR neurons were observed at the dorsoposterior tip of the central brain of both hemi-brains (Fig. 3D), here referred to as the dorsal posterior cells (DPCs). The DPCs show anti-ELAV staining (Fig. 3E). The DPC cluster has large cell bodies with FOR localized to the cytosol and/or plasma membrane (Fig. 3E). We did not observe FOR immunoreactivity in the axon projections of these neurons, and it is unclear to which region of the brain the axons of these cells might project.

Cluster #3: optic lobes. Bilateral clusters of FOR-IR neurons were observed in the region medial to the optic

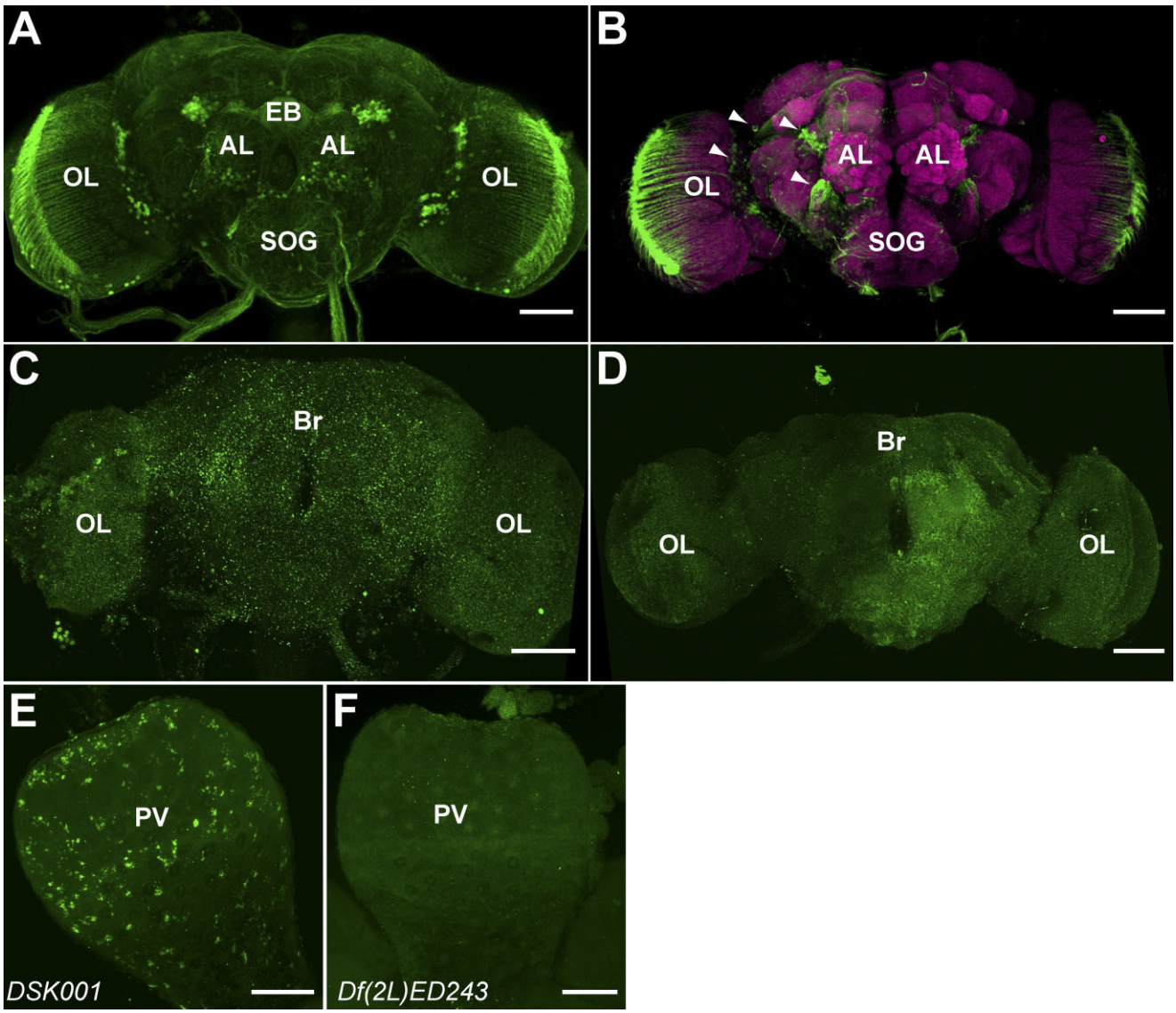

Fig. 2. FOR immunoreactivity (FOR-IR) in the brain. All brains are shown in a frontal view with dorsal at the top; the images are 3D reconstructions of 2-μm optical sections through the adult brain. FOR-IR regions are colored green. There are five anti-FOR immunoreactive clusters and fibers. Four of these cell clusters and projection nerves of the subesophagial ganglion (SOG) are visible in (**A**) and partly in (**B**). The locations of these clusters are shown relative to neuropiles within the central brain and the optic lobes (B), marked with anti-nc82 (magenta). **C,D:** Negative controls, for which FOR immunoreactivity was abolished following antibody adsorption (C), and weak ubiquitous staining that resulted from exposure of a specimen only to the secondary antibody (D). **E,F:** FOR-IR in larval *for* null tissue, the proventriculus (F) and its wildtype control (E). Images (anterior up) are 3D reconstruction of 2-μm optical sections spanning the whole proventriculus. (E) Punctate-like expression of FOR in the wild type control, *DSK001*, proventriculus epithelial cells. This staining pattern is absent in the mutant *Df(2L)ED243* (F). AL, antennal lobe; Br, brain hemisphere; EB, ellipsoid body; M, medulla; OL, optic lobe; PV, proventriculus, SOG, subesophageal ganglion. Scale bar = 50 μm.

lobes and lateral to the central brain (Fig. 3F, arrowhead). Due to the proximity to the optic lobes, these groups of neurons are referred to as optic lobe (OL) clusters. These cells are anti-ELAV-positive (Fig. 3G,G′). Neurons of the OL cluster can further be divided into those that show less intense nuclear staining and are found scattered (dorsoventrally) throughout the optic lobe/central brain region (OL neurons in Fig. 3F,G,G′, arrowhead) and those that show high-intensity staining and are located at the dorsal region, adjacent to the central brain (lateral cells [LC]; Fig. 3H,I, arrowheads). The LC group is made up of a single neuron in each brain hemisphere and showed strong cytoplasmic and/or plasma membrane-associated staining but no nuclear signals (Fig. 3I,I″). These neurons have the largest diameter (6–7 μm) of all of the FOR-IR cells observed in the adult brain.

FOR-IR frontal clusters and fiber-like projections.

Cluster #4: ventrofrontal. A group of sparsely distributed FOR-IR neurons was observed on the most anterior and frontal region of the brain, dorsal to the subesopha-

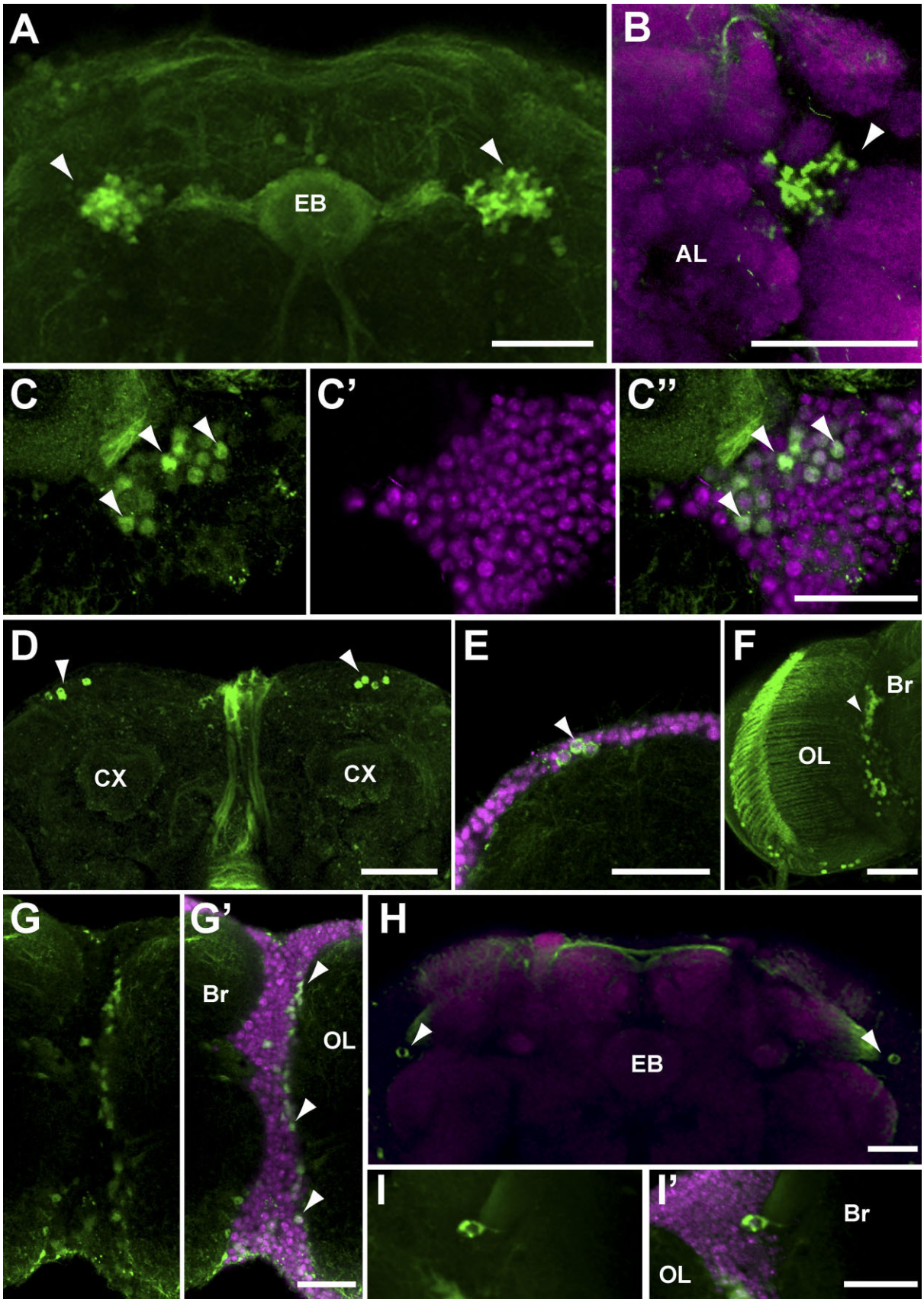

Figure 3

geal ganglia (SOG) and ventral to the antennal lobes (Fig. 4A, circled area). Images taken at higher magnification showed that FOR expression in these cells is localized to the nucleus (Fig. 4B, arrowhead). This was further supported by the colocalization between the FOR staining and the neuronal marker ELAV staining in the nucleus of these cells (Fig. 4B).

Cluster #5: medulla soma and fibers. Dense and fiber-like FOR-immunoreactivity was observed on the surface of the optic lobes (Fig. 4D) and lateral to the optic lobe clusters described above. This pattern of FOR expression was found in all individuals tested ($n > 50$) and was strong in intensity. This fiber-like expression pattern resembles that of the columnar arrangement of photoreceptor axons projecting to the medulla but does not show colocalization with these axons (data not shown). As one's perspective moves from the frontal region of the optic lobes posteriorly, the FOR-IR region becomes restricted to a crescent-like row of cells at the lateral region of the medulla, the outer medulla (Fig. 4E). This FOR-IR crescent region of the optic lobes is devoid of anti-ELAV labeling (Fig. 4E′,E″). It is not clear whether the cell bodies found at the lateral medulla are connected to the projections or fiber-like structures we observed at the outer frontal surface of the optic lobe or whether FOR is expressed in support sheet-like structures that make up the columnar structures of the optic lobes. The presence of FOR in the visual system of the fly suggests that FOR/PKG may play a role in the processing of visual information.

Pattern features #6 and #7: axonal projections of the central brain. Strong FOR-immunoreactivity was observed in axon bundles that enter the brain hemispheres just ventrolateral to the antennal lobes (AL) (Fig. 2B). Brain tissue preparations in which the antennal nerve (AN) ($n > 8$) was left attached to the brain showed strong staining in the AN (Fig. 4C). Furthermore, we observed strong FOR expression at the entrance point of the AN to the brain (Fig. 4C′) It was clear that the majority of these FOR-expressing nerves terminated posteroventral to the AL in a brain region known as the antennal mechanosensory region or the antennal mechanosensory and motor center (Kamikouchi et al., 2006). This region of the brain is the first-order relay point for auditory and other mechanosensory cues, such as gravity sensing, suggesting a role for FOR in the processing of auditory and/or nonauditory mechanosensory information. Furthermore, we cannot rule out possible function of FOR in olfactory signaling, as some of the FOR-expressing antennal nerve fibers may project to the antennal lobes. Sensory neurons of the antennae were not observed to label with anti-FOR (data not shown).

FOR immunoreactivity was also observed in a pair of nerves that innervates the SOG (Figs. 2A, 4A, arrowhead). There are three nerves that innervate the SOG, and this may be one of the three neurites that carries chemosensory signals from the labial region to the SOG, where such information is processed (Stocker and Schorderet, 1981). A schema of the FOR-IR cellular patterns is shown in Figure 4F (the FOR-IR fiber-like projections are not included in this schematic).

In addition to the FOR-IR regions described above, we observed diffuse expression throughout the brain but most frequently in the mushroom-body neuropiles, the calyx, and the CC, specifically in the ellipsoid body. Although our antibody did not result in as clean labeling of the ventral ganglia as presented here for the brain, we observed a few clusters of FOR-IR cells in the ventral ganglia (data not shown). Examination of the sensory neurons of the tarsi, wings, and proboscis ($n = 10–15$) peripheral structures that could be related to SR, did not show FOR immunoreactivity. We cannot rule out the possibility that whole-mount immunohistochemistry may not allow the FOR antibody to penetrate the hard peripheral tissues, although in a similar procedure using anti-elav antibody we observed clear labeling in the sensory neurons of the proboscis.

Expression of *for* in neurons causes an increase in the sucrose responsiveness of sitter flies

We assayed the head and body PKG enzyme activities of for^R, for^s, and for^{s2} flies using a modified assay from Osborne et al. (1997) and confirmed that these lines show differences in PKG enzyme activities. Rovers exhibit significantly higher PKG enzyme activities than sitters in their heads (Fig. 5; ANOVA, $F_{(2,11)} = 37.05$, $P < 0.0001$). PKG activities were generally lower in the bodies than heads. In the fly body we found no difference in PKG enzyme activities between the natural rover and sitter strains and a reduction in activity in the bodies of the sitter mutant (for^{s2}) *(Fig. 5; ANOVA,* $F_{(2,11)} = 33.09$, $P <$ 0.0001).

Sitter flies have lower PKG activities than rovers and increasing *for-T2* expression in sitter larvae alters a suite of foraging-related behaviors to that of a rover (Osborne et al., 1997; Kaun et al., in press). We expressed *for-T1* and *for-T2* in sitter neurons to induce a rover-like SR. (For now, *for*-T3 was not used because the T3 transcript is a complete subset of T1.) This was accomplished using the *Drosophila* GAL4/UAS system (Brand and Perrimon, 1993). Sex did not significantly affect SR in these experiments, so behavioral data from males and females were pooled. Increasing expression of *for* transgenes (encoding

Fig. 3. Detailed features of FOR-immunoreactive clusters. Anti-FOR mediated signals are in green, neuropile marking (elicited by mAb nc82) in magenta in B and H, and nuclear neuronal ELAV immunoreactivity in magenta in C′, C″, E, and G′. **A:** 3D reconstruction of 2-μm sections spanning cluster #1 (EB) cells shows FOR is expressed in somata located lateral to the ellipsoid body (EB). These cells send fiber-like projections to the central complex. **B:** The EB cluster is located just anterior-lateral to the ALs. **C–C″:** A single optical section through this cluster of cells shows FOR-immunoreactive is localized to the nucleus of anti-ELAV positive cells (for example, see arrowheads). **D:** Posterior view showing 3D reconstruction of sections spanning cluster #2 (DPC), 4–5 FOR-IR cells located at the dorsal posterior margins of the brain hemispheres. **E:** Single 2-μm section taken at higher magnification shows FOR localization to the plasma membrane and/or cytosol of these neurons. **F:** Cluster #3 (OL) shows a number of FOR-IR cells located between the brain hemisphere and optic-lobe regions (arrowhead). These cells are distributed dorsoventrally in this region and show colocalization with a neural marker (**G,G′,** single section). Cluster #3 also consists of a single large cell (LC) found at the dorsolateral region of the brain-hemisphere/optic-lobe boundary (**H,** arrowheads); these cells are relatively large and show expression in the cytosol/plasma membrane and are neurons (**I,I′,** single section). AL, antennal lobe; Br, brain hemisphere; CX mushroom body calyx; EB, ellipsoid body; LC, lateral cell; M, medulla; OL, optic lobe. Scale bars = 50 μm in A,B,D,F; 25 μm in C″,E,G′,H,I′.

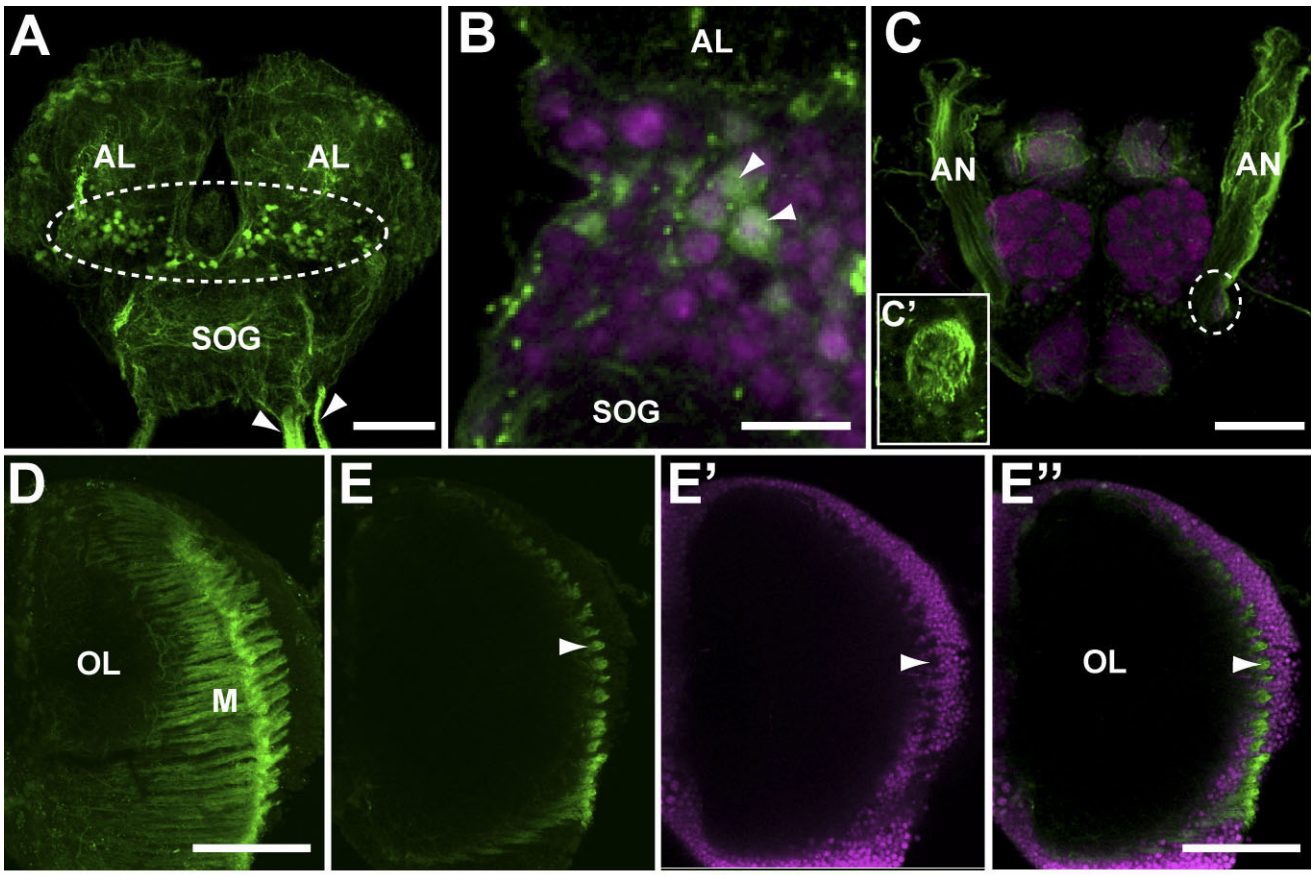
A
AL
AL
SOG
B
AL
SOG
C
AN
AN
C'
D
OL
M
E
E'
E''
OL

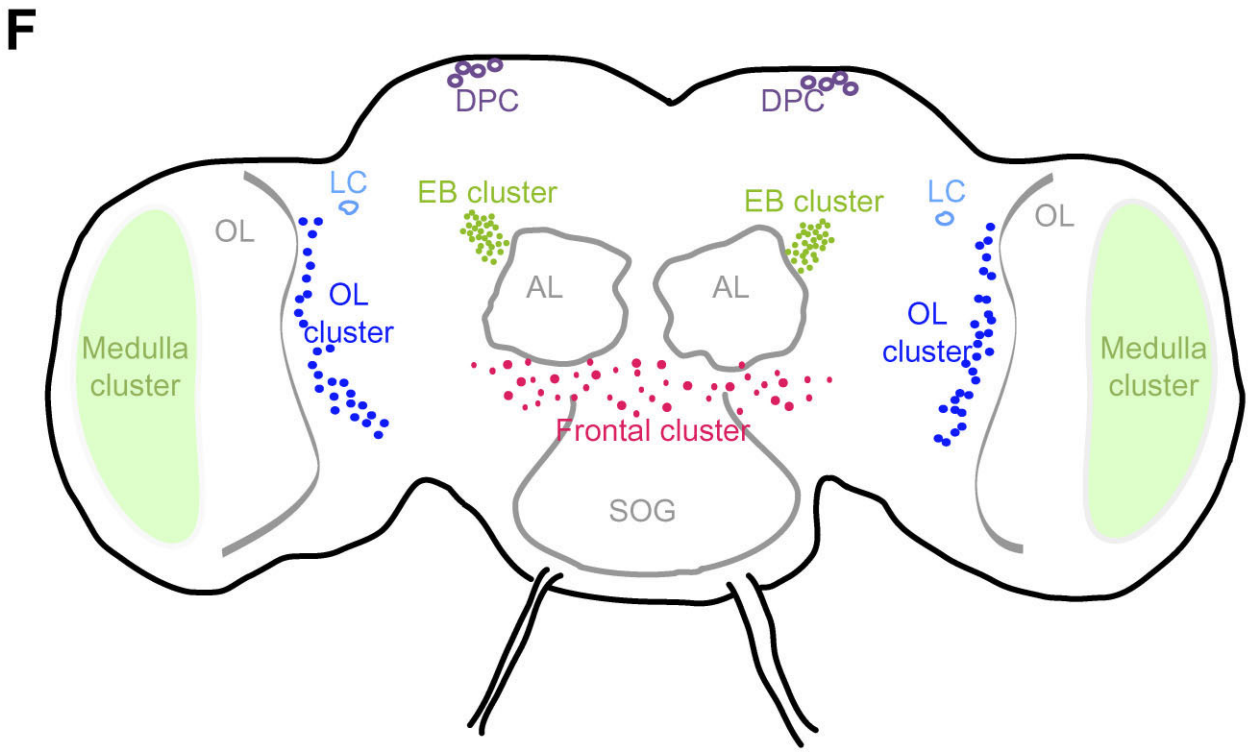
F
DPC
DPC
LC
EB cluster
EB cluster
LC
OL
OL
AL
AL
OL cluster
OL cluster
Medulla cluster
Medulla cluster
Frontal cluster
SOG

Figure 4

either T1 or T2 transcript types) in sitter neurons significantly increased SR (Fig. 6). Specifically, *elav-gal4*/UAS-*forT1* flies showed significantly higher SR than their respective controls: w^1;for^s;UAS-*forT1*/+ and w^1;for^s;*elav-gal4*/+ (ANOVA, $F_{(2,597)} = 12.18$, $P \leq 0.0001$) (Fig. 6A,C). Similarly, neuronal expression of the *forT2* transcript caused an increase in SR of sitters relative to their respective controls (Fig. 6B,D; ANOVA, $F_{(2,597)} = 66.36$, $P \leq 0.0001$). This increased responsiveness of sitters was observed for both 2-hour (Fig. 6C,D) and 24-hour (Fig. 6A,B) food-deprivation treatments and, as expected (Scheiner et al., 2004b), flies were more responsive to sucrose after 24 hours compared with 2 hours of food deprivation (Fig. 6A,B: ANOVA, $F_{(1,598)} = 321.85$, $P \leq 0.0001$; and Fig. 5C,D: ANOVA, $F_{(1,598)} = 301.14$, $P \leq 0.0001$). Typically, for^R flies show average SR scores of 4 following a 24-hour food deprivation and 2 following 2 hours of food deprivation (Scheiner et al., 2004b); this suggests that expression of *for* in sitter neurons with the *elav-gal4* driver did not fully restore SR to rover levels (rescue to rover SR ranged from 65–85% for T2 and from 35–70% with T1 under conditions of 2-hour and 24-hour food deprivation, respectively). Although both the T1 and T2 transcripts significantly increased SR when expressed in neurons, the T2 transcript appeared to have a larger effect on SR (Fig. 6). Furthermore, Western blot analysis of head extracts of the double transgenic strains showed an increase in band intensity of the corresponding isoform compared to that of the control strains. The *elav-gal4*/UAS-*forT2* strain showed 4.4- and 6.9-fold increases in T2 band intensity compared to the UAS-*forT2* and *elav-gal4* controls, respectively. We conclude that neuronal expression of *for* in sitters is sufficient to increase SR; this increase in SR can be achieved with either the T1 or T2 isoforms, indicating that either isoform may function on behalf of sucrose responsiveness.

Fig. 4. FOR-IR clusters #4–7 and schematic of FOR-IR brain regions. FOR immunoreactivity is shown in green and magenta represents immunoreactivity to the neural marker anti-ELAV in B,E′, E″ and to the neuropile marker, nc82, in C. **A:** Cluster #4 (ventrofrontal) consists of FOR-immunoreactive cells distributed across the frontal surface of the brain in the region between the AL and SOG neuropiles (A, circled region). **B:** Single section image through cluster #4 shows FOR-IR is localized to the nucleus of theses cells and the cells are neuronal (arrowhead, single section). FOR is also expressed in fiber-like projections in the AN (**C**) and projection nerves of the SOG (arrowheads in A). Insert in C,C′ shows FOR localization at the brain entry point of the AN (circled in C). Cluster #5 (medulla) shows FOR expression in a fiber-like structure distributed across the optic lobes (**D,** 3D reconstruction of sections spanning the optic lobe). **E:** A single section through this region shows a crescent-like expression at the lateral region of the lobes; these cells are not positive for the neural marker, anti-ELAV (E′,E″). **F:** Schematics of FOR-IR clusters in the adult brain: #1 (ellipsoid body [EB] cluster), #2 (DPC cluster), #3 (OL/LC cluster), #4 (frontal cluster), and #5 (medulla cluster, in an optic lobe flanking the brain per se). The schematic represents the spatial pattern of FOR expressing cellular clusters but not the projection patterns and the number of cells shown on schematics do not necessarily represent actual number of cells in a cluster. AL, antennal lobe; AN, antennal nerve; Br, brain hemisphere; DPC, dorsal-posterior cells; EB, ellipsoid body; LC, lateral cell; M, medulla; OL, optic lobe; SOG, subesophageal ganglion. Scale bars = 50 μm in A,C–E; 10 μm in B.

DISCUSSION

Our characterization of PKG expression patterns in *D. melanogaster*, a genetically tractable organism, is an important and essential advance toward the understanding of cellular functions of PKGs. We describe, for the first time, the brain distribution pattern of FOR in the adult fruitfly, *D. melanogaster*. We also show that increasing the level of FOR in neurons is sufficient to increase SR in sitters. In mammals, subcellular localization of PKG isoforms is found in different subcompartments of the cell (for example, see Feil et al., 2005). Similarly, in adult tissues of *Drosophila*, FOR is expressed in the nuclei of some cells (the EB, OL, and ventrofrontal clusters), while it is highly enriched in the cytoplasm and/or plasma membrane (the LC and DPC clusters) of other cells. MacPherson et al. (2004) showed that in *Drosophila* S2 cell cultures, T1- and T2-encoded isoforms of FOR were localized to the plasma membrane of the cells. Our antibody detects all three of *for*'s major protein isoforms. Immunohistochemical analyses with this antibody showed that rovers and sitters do not have obvious differences in FOR spatial distribution. Further studies using FOR isoform-specific antibodies will allow for a detailed comparison of the patterns and levels of FOR expression.

Although in the past we have shown that adult heads have PKG kinase activity, we did not know if only some or all isoforms are expressed in the adult brain. Our results, for the first time, show that all three isoforms are expressed in the adult brain. It is possible that all or only some of these FOR isoforms explain the kinase activity differences between rovers and sitters. Our preliminary results demonstrate that there are isoform-specific contributions to differences in PKG enzyme activities (A. So, unpubl. data). Furthermore, MacPherson et al. (2004) showed that some of the FOR isoforms differ in EC50 for cGMP binding; cGMP binding to PKGs initiates a cascade of events that leads to activation of the kinase. It is possible that there are differences in the activity levels of each of the isoforms and/or that the rover PKG variants are more readily activated than the sitter ones. These relationships remain to be further elucidated. Finally, sequence differences between these variants have not yet been investigated.

Mammalian studies have shown that the different products of PKG-expressing genes, cGKI and cGKII, show distinct localization patterns in some regions of the mammalian brain, while other regions may express both gene products but at different levels (Schlossmann and Hofmann, 2005; Hofmann et al., 2006). This leads to the question of how isoform- and tissue-specific expression patterns relate to *for*'s pleiotropic functions. However, the patterns of FOR immunoreactivity that we observed seem to correlate with the roles *for* plays in physiology and behavior (Renger et al., 1999).

Immunohistochemical analysis using our common antibody did not uncover differences in abundance of protein in the heads of rovers, sitters, and sitter mutants. Detailed analysis with isoform-specific FOR antibodies is required to assess possible differences in the spatial expression patterns or level of expression patterns of the FOR isoforms in rovers and sitters. Interestingly, either the T1 or the T2 transcript could be used in neurons to increase SR from a sitter to a rover-like level. Investigating the differences in spatial expression patterns of T1

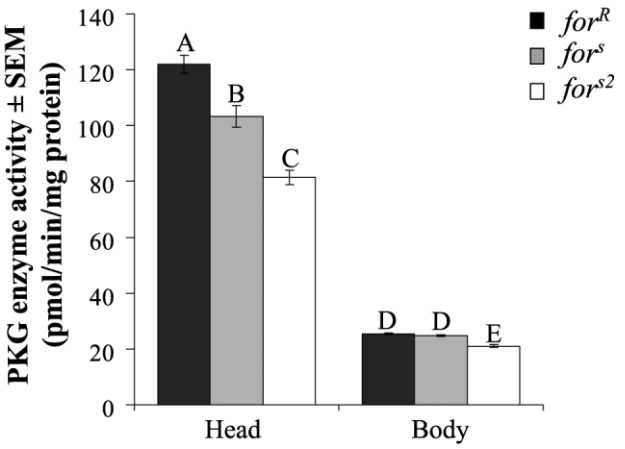

Fig. 5. PKG enzyme activity levels in rover and sitter flies. Rover (*for*^{R}) head extracts show significantly higher PKG activities than those of sitters (*for*^{s} and *for*^{s2}). All three strains show relatively lower levels of PKG activity in the bodies than in the heads. The bodies of rovers and sitters do not differ in PKG activity. The sitter mutant (*for*^{s2}) shows significantly lower PKG activity than *for*^{R} and *for*^{s} in the head and body. Four independent protein extractions and activity measures were performed and the mean of these values is presented (letters indicate significant differences according to Tukey's post-hoc comparisons at $P = 0.05$).

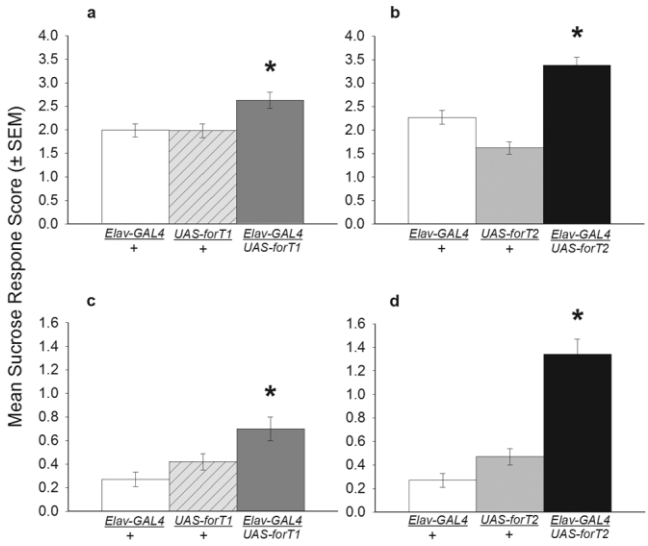

Fig. 6. Sucrose responsiveness (SR) increases when either the *for* T1 or T2 transcript is expressed in the nervous system of sitter flies using the *elav*-GAL4 driver. Mean SRS ± SE of 1-week-old flies deprived of food for 24 hours (**A,B**) or 2 hours (**C,D**) are shown. Expression of either the *forT1* (A,C) or the *forT2* (B,D) transgene under the control of *elav*-GAL4 driver caused a significant increase in the SR score of sitters relative to the controls under 24-hour (A,B) and 2-hour (C,D) food deprivations; 50 males and 50 females were tested/strain.

and T2 protein isoforms in rover and sitters may shed light on the cellular mechanism governing SR. Furthermore, isoform-specific localizations of T1 and T2 will aid in identifying the neural cluster(s) involved in SR.

FOR may be involved in the regulation of gustatory responsiveness in *Drosophila,* which in turn could affect behaviors such as food intake and food choice. Increasing *for* in sitter neurons increases SR. SR in the adult fruitfly likely involves pathways that detect sucrose via the gustatory receptors found in sensory neurons (e.g., the tarsi) and transmit the information to the gustatory region of the thoracic-abdominal ganglion, which somehow causes the fly to respond by extending its proboscis. Nerves carry the gustatory information detected by the proboscis to the SOG, the first relay point of the processing of gustatory information in the adult fly brain (Stocker, 1994). Information may then be sent to a higher-order brain region for interpretation of gustatory information, as in the honeybee (Schroter and Menzel, 2003). This region could integrate relevant food-related sensory stimuli and thus be involved in the regulation of SR. *for* could affect SR at any one or a combination of the above pathways. One candidate region for FOR's regulation of SR is the cluster of FOR-immunoreactive cells that project axons to the EB of the CC, thought to be an information integration center in the fly brain (Heisenberg, 1994). FOR expression in these neurons may modulate gustatory information received via the peripheral chemosensory organs and thereby affect the proboscis-extension response.

The efferent nerves of the SOG thought to be involved in gustation could also be involved in SR. A pair of nerves that project from the proboscis to this ventral-brain region shows FOR expression. Axons of gustatory receptor neurons found in the labellum project to distinct regions of the SOG via the labial nerves (Stocker and Schorderet, 1981; Nayak and Singh, 1985) and projections from sensory neurons of the internal mouthparts, labral sense organ, and the cibarial sense organs reach the SOG via the pharyngeal and the accessory pharyngeal nerves, respectively. FOR's possible presence in the labial nerve would be in line with its role in food-related phenotypes. Interestingly, we also found a high level of FOR expression in the antennal nerve of the fly. The antennal nerve carries axons of the olfactory, auditory, and mechanosensory neurons (Stocker, 1994). It remains to be determined whether FOR's expression in the antennal nerve is associated with one or all of these types of neurons. FOR was also found in the OL of the fly, suggesting a function in reception and/or processing of visual stimuli, as has been suggested for the honeybee *Amfor* gene (Ben-Shahar et al., 2003). Interestingly, the mammalian FOR homolog is expressed at a high level in the mouse eye (Gamm et al., 2000). Furthermore, cGKI was shown to be expressed in the hypothalamus and the pituitary gland, regions of the brain known to influence food intake and body weight regulation (Schwartz et al., 2000; Bellinger and Bernardis, 2002).

It remains to be determined which tissues are required for each of *for*'s food-related phenotypes. Furthermore, it is not known whether FOR is needed acutely and/or during development for rover/sitter differences in behavior. Our transgenic studies of SR in sitters and our initial characterization of FOR protein expression in adults represent an important and essential advance toward understanding how PKG functions in food-related behaviors.

ACKNOWLEDGMENTS

We thank Jeff Hall and John Ewer for guidance, J. Krupp, members of the Sokolowski lab, and anonymous

reviewers for valuable comments and M. Busto for help with Figure 6. We also thank the Bloomington and Szeged Fly Stock Centers for fly lines and A. Hofbauer for nc82 antibody.

LITERATURE CITED

Bellinger LL, Bernardis LL. 2002. The dorsomedial hypothalamic nucleus and its role in ingestive behavior and body weight regulation: lessons learned from lesioning studies. Physiol Behav 76:431–442.

Ben-Shahar Y, Leung HT, Pak WL, Sokolowski MB, Robinson GE. 2003. cGMP-dependent changes in phototaxis: a possible role for the foraging gene in honey bee division of labor. J Exp Biol 206(Pt 14): 2507–2515.

Brand AH, Perrimon N. 1993. Targeted gene expression as a means of altering cell fates and generating dominant phenotypes. Development 118:401–415.

Campbell G, Goring H, Lin T, Spana E, Andersson S, Doe CQ, Tomlinson A. 1994. RK2, a glial-specific homeodomain protein required for embryonic nerve cord condensation and viability in Drosophila. Development 120:2957–2966.

de Belle JS, Sokolowski MB. 1987. Rover/sitter foraging behavior in Drosophila melanogaster: genetic localization to chromosome-2L using compound autosomes. J Insect Behav 2:291–299.

de Belle JS, Hilliker AJ, Sokolowski MB. 1989. Genetic localization of foraging (for): a major gene for larval behavior in Drosophila melanogaster. Genetics 123:157–163.

Dethier V. 1955. The physiology and histology of the contact chemoreceptors of the blowfly. Q Rev Biol 30:348–371.

Douglas SJ, Dawson-Scully K, Sokolowski MB. 2005. The neurogenetics and evolution of food-related behaviour. Trends Neurosci 28:644–652.

Erber J, Hoormann J, Scheiner R. 2006. Phototactic behaviour correlates with gustatory responsiveness in honey bees (Apis mellifera L.). Behav Brain Res 174:174–180.

Feil S, Zimmermann P, Knorn A, Brummer S, Schlossmann J, Hofmann F, Feil R. 2005. Distribution of cGMP-dependent protein kinase type I and its isoforms in the mouse brain and retina. Neuroscience 135:863–868.

Fitzpatrick MJ, Ben-Shahar Y, Smid HM, Vet LE, Robinson GE, Sokolowski MB. 2005. Candidate genes for behavioural ecology. Trends Ecol Evol 20:96–104.

Gamm DM, Barthel LK, Raymond PA, Uhler MD. 2000. Localization of cGMP-dependent protein kinase isoforms in mouse eye. Invest Ophthalmol Vis Sci 41:2766–2773.

Green RB, Hatini V, Johansen KA, Liu XJ, Lengyel JA. 2002. Drumstick is a zinc finger protein that antagonizes lines to control patterning and morphogenesis of the Drosophila hindgut. Development 129:3645–3656.

Greenspan RJ. 2004. E pluribus unum, ex uno plura: quantitative and single-gene perspectives on the study of behavior. Annu Rev Neurosci 27:79–105.

Hall JC. 2003. A neurogeneticist's manifesto. J Neurogenet 17:1–90.

Halter DA, Urban J, Rickert C, Ner SS, Ito K, Travers AA, Technau GM. 1995. The homeobox gene repo is required for the differentiation and maintenance of glia function in the embryonic nervous system of Drosophila melanogaster. Development 121:317–332.

Heisenberg M. 1994. Central brain function in insects: genetic studies on the mushroom bodies and central complex in Drosophila. In: Schildberger K, editor. Neural basis of behavioral adaptations. Stuttgart: Gustav Fisher. p 61–79.

Hofbauer A. 1991. Eine Bibliothek monoklonaler Antikörper gegen das Gehirn von Drosophila melanogaster. Habilitation thesis, Würzburg, Germany: University of Würzburg.

Hofmann F, Feil R, Kleppisch T, Schlossmann J. 2006. Function of cGMP-dependent protein kinases as revealed by gene deletion. Physiol Rev 86:1–23.

Kalderon D, Rubin GM. 1989. cGMP-dependent protein kinase genes in Drosophila. J Biol Chem 264:10738–10748.

Kamikouchi A, Shimada T, Ito K. 2006. Comprehensive classification of the auditory sensory projections in the brain of the fruit fly Drosophila melanogaster. J Comp Neurol 499:317–356.

Kaun KR, Riedl CAL, Chaterjee MC, Belay AT, Douglas SJ, Gibbs AG, Sokolowski MB. Natural variation in food acquisition mediated via a Drosophila cGMP-dependent protein kinase. J Exp Biol (in press).

Lin DM, Goodman CS. 1994. Ectopic and increased expression of Fasciclin II alters motoneuron growth cone guidance. Neuron 13:507–523.

MacPherson MR, Lohmann SM, Davies SA. 2004. Analysis of Drosophila cGMP-dependent protein kinases and assessment of their in vivo roles by targeted expression in a renal transporting epithelium. J Biol Chem 279:40026–40034.

Nayak SV, Singh RN. 1985. Primary sensory projections from labella to the brain of Drosophila melanogaster Meigen (Diptera: Drosophilidae). Int J Insect Morphol Embryol 14:115–129.

O'Neill EM, Rebay I, Tjian R, Rubin GM. 1994. The activities of two Ets-related transcription factors required for Drosophila eye development are modulated by the Ras/MAPK pathway. Cell 78:137–147.

Osborne KA, Robichon A, Burgess E, Butland S, Shaw RA, Coulthard A, Pereira HS, Greenspan RJ, Sokolowski MB. 1997. Natural behavior polymorphism due to a cGMP-dependent protein kinase of Drosophila. Science 277:834–836.

Pereira HS, Sokolowski MB. 1993. Mutations in the larval foraging gene affect adult locomotory behavior after feeding in Drosophila melanogaster. Proc Natl Acad Sci U S A 90:5044–5046.

Rein K, Zockler M, Heisenberg M. 1999. A quantitative three-dimensional model of the Drosophila optic lobes. Curr Biol 9:93–96.

Renger JJ, Yao WD, Sokolowski MB, Wu CF. 1999. Neuronal polymorphism among natural alleles of a cGMP-dependent kinase gene, foraging, in Drosophila. J Neurosci 19:RC28.

Renn SC, Armstrong JD, Yang M, Wang Z, An X, Kaiser K, Taghert PH. 1999. Genetic analysis of the Drosophila ellipsoid body neuropil: organization and development of the central complex. J Neurobiol 41:189–207.

Ryder E, Blows F, Ashburner M, Bautista-Llacer R, Coulson D, Drummond J, Webster J, Gubb D, Gunton N, Johnson G, O'Kane CJ, Huen D, Sharma P, Asztalos Z, Baisch H, Schulze J, Kube M, Kittlaus K, Reuter G, Maroy P, Szidonya J, Rasmuson-Lestander A, Ekstrom K, Dickson B, Hugentobler C, Stocker H, Hafen E, Lepesant JA, Pflugfelder G, Heisenberg M, Mechler B, Serras F, Corominas M, Schneuwly S, Preat T, Roote J, Russell S. 2004. The DrosDel collection: a set of P-element insertions for generating custom chromosomal aberrations in Drosophila melanogaster. Genetics 167:797–813.

Sambrook J, Russell DW. 2001. Molecular cloning: a laboratory manual. New York: Cold Spring Harbor Laboratory Press.

Samson ML, Lisbin MJ, White K. 1995. Two distinct temperature-sensitive alleles at the elav locus of Drosophila are suppressed nonsense mutations of the same tryptophan codon. Genetics 141:1101–1111.

Scheiner R. 2004. Responsiveness to sucrose and habituation of the proboscis extension response in honey bees. J Comp Physiol A Neuroethol Sens Neural Behav Physiol 190:727–733.

Scheiner R, Erber J, Page RE Jr. 1999. Tactile learning and the individual evaluation of the reward in honey bees (Apis mellifera L.). J Comp Physiol [A] 185:1–10.

Scheiner R, Page RE Jr, Erber J. 2001a. The effects of genotype, foraging role, and sucrose responsiveness on the tactile learning performance of honey bees (Apis mellifera L.). Neurobiol Learn Mem 76:138–150.

Scheiner R, Page RE Jr, Erber J. 2001b. Responsiveness to sucrose affects tactile and olfactory learning in preforaging honey bees of two genetic strains. Behav Brain Res 120:67–73.

Scheiner R, Page RE, Erber J. 2004a. Sucrose responsiveness and behavioral plasticity in honey bees (Apis mellifera). Apidologie 35: 133–142.

Scheiner R, Sokolowski MB, Erber J. 2004b. Activity of cGMP-dependent protein kinase (PKG) affects sucrose responsiveness and habituation in Drosophila melanogaster. Learn Mem 11:303–311.

Scheiner R, Kuritz-Kaiser A, Menzel R, Erber J. 2005. Sensory responsiveness and the effects of equal subjective rewards on tactile learning and memory of honeybees. Learn Mem 12:626–635.

Schlossmann J, Hofmann F. 2005. cGMP-dependent protein kinases in drug discovery. Drug Discov Today 10:627–634.

Schroter U, Menzel R. 2003. A new ascending sensory tract to the calyces of the honeybee mushroom body, the subesophageal-calycal tract. J Comp Neurol 465:168–178.

Schwartz MW, Woods SC, Porte D Jr, Seeley RJ, Baskin DG. 2000. Central nervous system control of food intake. Nature 404:661–671.

Singh RN. 1997. Neurobiology of the gustatory systems of Drosophila and some terrestrial insects. Microsc Res Tech 39:547–563.

Skaer H. 1993. The alimentary canal. In: Bate MaM, Arias A, editors. The development of Drosophila melanogaster. Cold Spring Harbor, NY: Cold Spring Harbor Laboratory Press. p 941–1012.

So AK-C, Espie GS. 1998. Cloning, characterization and expression of carbonic anhydrase from the cyanobacterium Synechocystis PCC6803. Plant Mol Biol 37:205–215.

So AK-C, Cot SS-W, Espie GS. 2002. Characterization of the C-terminal extension of carboxysomal carbonic anhydrase from Synechocystis sp. PCC6803. Funct Plant Biol 29:183–194.

Sokolowski MB. 1980. Foraging strategies of Drosophila melanogaster: a chromosomal analysis. Behav Genet 10:291–302.

Sokolowski MB. 2001. Drosophila: genetics meets behaviour. Nat Rev Genet 2:879–890.

Spradling AC. 1986. P element-mediated transformation. Roberts DB, editor. Oxford: IRL Press.

Stocker RF. 1994. The organization of the chemosensory system in Drosophila melanogaster: a review. Cell Tissue Res 275:3–26.

Stocker RF, Schorderet M. 1981. Cobalt filling of sensory projections from internal and external mouthparts in Drosophila. Cell Tissue Res 216: 513–523.

Strauss R. 2002. The central complex and the genetic dissection of locomotor behaviour. Curr Opin Neurobiol 12:633–638.

Varnam CJ, Strauss R, Belle JS, Sokolowski MB. 1996. Larval behavior of Drosophila central complex mutants: interactions between no bridge, foraging, and Chaser. J Neurogenet 11:99–115.

Wagh DA, Rasse TM, Asan E, Hofbauer A, Schwenkert I, Durrbeck H, Buchner S, Dabauvalle MC, Schmidt M, Qin G, Wichmann C, Kittel R, Sigrist SJ, Buchner E. 2006. Bruchpilot, a protein with homology to ELKS/CAST, is required for structural integrity and function of synaptic active zones in Drosophila. Neuron 49:833–844.

Zar JH. 1999. Biostatistical analysis. Englewood Cliffs, NJ: Prentice Hall. p 312–323.